Photonics Breakthroughs 2024: Arbitrary Mode Manipulation Using Reconfigurable Integrated Photonic Processors

SeyedMohammad SeyedinNavadeh, *Member, IEEE*, Francesco Zanetto, *Member, IEEE*, Andres Ivan Martinez, Giorgio Ferrari, *Member, IEEE*, David A. B. Miller, *Life Fellow, IEEE*, Andrea Melloni, *Member, IEEE*, and Francesco Morichetti, *Member, IEEE*

***Abstract*—Optical modes offer spatial degrees of freedom that can be exploited to implement advanced functionalities across various applications. Conventional photonic devices used for the manipulation of modes operate on predetermined families of eigenmodes of specific systems. Here, we report on a recent finding of our research, where we demonstrate that reconfigurable photonic integrated circuits (PICs) can automatically identify optimal communication modes through arbitrary systems, always ensuring maximum achievable power transmission and mutual orthogonality. Such modes are determined in situ without any precalculation or prior knowledge of the system. Our results extend the concepts and the range of applications of existing schemes for mode manipulation to more complex functionalities and realistic scenarios. We also address recent related works on reconfigurable PICs for generation and detection of arbitrary, structured, and random beams, with an overview of the main results achieved on the different free-space and guided-waves technologies. A discussion of the main limits of the presented approach and the potential implications in diverse and emerging application fields is provided.**

***Index Terms*—Photonic integrated circuits (PICs), optical modes, reconfigurable photonics, mach-zehnder interferometers, integrated photonic processors, spatial division multiplexing (SDM).**

I. Introduction

THE propagation of light in an optical medium occurs according to optical modes, where the "modes" are typically defined as the eigen-solutions of the wave equation that holds in a given system. In other words, the modes provide the spatial degrees of freedom of the system. A direct consequence is that, by manipulating the way light beams map onto the available modes, one can implement advanced functionalities exploitable in a plethora of different fields of application. Probably the best example is given by communications in fiber optics, where the leveraging of the spatial modes of few-mode fibers (FMFs), multi-core fibers, and multimode fibers has emerged as an effective solution to overcome the capacity limitations of single-mode fiber links. The same concept is applicable to free-space optics, where encoding parallel data channels on orthogonal modes, such as Laguerre-Gaussian (LG) modes or orbital angular momentum (OAM) modes, is being actively explored to increase data capacity per wavelength. Besides communications, there are many other fields where high-order modes can be exploited, such as imaging and spectroscopy, multi-parameter sensing, integrated communication and sensing, classical and quantum photonic computing, and beam combination for very high-power lasers.

Fully exploiting the degrees of freedom offered by optical modes requires devices capable of manipulating these modes, converting one mode into another, while preserving their mutual orthogonality. When the modes of the system are known in advance and remain stable over time, passive mode converters can be designed and fabricated using various technologies, such as bulk free-space optics, optical fibers, and integrated photonics. If the mode sets at the input and at the output of the system are known, but their mapping has to be modified on demand, reconfigurable mode converters and/or mode sorters are required. However, there are many practical scenarios where the modes of a system are not predetermined; this could happen when the light propagates through highly complex scattering or time-varying media. In such cases, the concept of "mode" itself becomes more subtle. Instead of being associated with a predefined field configuration, modes must be identified as the optimal communication channels that efficiently transfer information between sets of input and output apertures across the system, while remaining orthogonal.

Determining such modes could appear to be a difficult task that might not even be feasible; however, a solution does exist. Recently, we provided an experimental validation of a concept that was proposed in 2013 by D.A.B. Miller [1], demonstrating that a pair of reconfigurable photonic integrated circuits

Received 17 March 2025; revised 28 April 2025; accepted 30 April 2025. Date of publication 5 May 2025; date of current version 21 May 2025. This work was supported in part by Italian National Recovery and Resilience Plan (NRRP) of NextGenerationEU, partnership on 'Telecommunications of the Future' (PE00000001—Program 'RESTART', Structural Project 'Rigoletto' and Focused Project 'HePIC') and by AFOSR under Grant FA9550.21.1.0312. *(Corresponding author: Francesco Morichetti.)*

SeyedMohammad SeyedinNavadeh, Francesco Zanetto, Andres Ivan Martinez, Andrea Melloni, and Francesco Morichetti are with Dipartimento di Elettronica, Informazione e Bioingegneria, Politecnico di Milano, 20133 Milano, Italy (e-mail: francesco.morichetti@polimi.it).

Giorgio Ferrari is with Dipartimento di Fisica, Politecnico di Milano, 20133 Milano, Italy.

David A. B. Miller is with Ginzton Laboratory, Stanford University, Stanford, CA 94305 USA.

Digital Object Identifier 10.1109/JPHOT.2025.3567203

© 2025 The Authors. This work is licensed under a Creative Commons Attribution 4.0 License. For more information, see https://creativecommons.org/licenses/by/4.0/

(PIC) can establish multiple communication channels through orthogonal spatial modes when propagating through arbitrary complex and even time-varying media [3]. These channels are automatically identified without any prior knowledge of the medium in between, by following a simple power optimization process, with no need for prior calibration or pre-calculated adjustments. These modes have arbitrary shapes that do not belong to any predetermined family of modes; however, they are the "true communication modes [2]" of the system.

This paper is organized as follows. In Section II, we summarize the main concepts and results of our research on the integrated photonic system that we used to determine the optimal modes of an arbitrary medium. Then, in Section II-B, we provide an overview of related works published in 2024 on the use of integrated photonic processors for the manipulation of fiber modes and free-space modes. Section II-C extends the discussion to the different technologies (optical fibers, free space, and integrated photonics) that have been used to implement passive and reconfigurable mode converters. A concluding section provides discussions on the limits of existing solutions and the potential impact of our research.

II. Breakthrough Research

A. Finding the Best-Coupled Modes of an Arbitrary Optical System Using a Pair of Integrated Photonic Processors

1) Concept and Principle:

a) SVD Modes: Any linear optical system with finite numbers M of input apertures and N of output apertures can be described by a transmission matrix $\mathbf{M_c}_{[N\times M]}$, which depends on the optical and geometrical properties of the medium in between and the number and position of the apertures. The modes of the system can be defined as the pairs of orthogonal input fields and corresponding orthogonal output fields that provide the highest power coupling through the system. They can be referred to as the "best-coupled" or "communication" [2] modes of the system, using which the orthogonal communication channels between inputs and outputs can be established. Mathematically, such modes can be obtained by calculating the singular-value decomposition (SVD) of $\mathbf{M_c}$ [2]

$$\mathbf{M_c} = \mathbf{V}\mathbf{\Sigma}\mathbf{U}^{\dagger} \tag{1}$$

where $\mathbf{U}_{[M\times M]}$ and $\mathbf{V}_{[N\times N]}$ are unitary matrices containing the "SVD mode-pairs" in the input and output space, i.e., the orthogonal sets $\{\psi_{\mathbf{u}_m}\}_{m=1}^{M}$ and $\{\phi_{\mathbf{v}_n}\}_{n=1}^{N}$, respectively, and $\mathbf{\Sigma}_{[N\times M]}$ is a diagonal matrix containing singular values or coupling strengths of these mode pairs, i.e., σ_k, with $k = \{1, \ldots, r = \mathrm{rank}\,\mathbf{M_c}\}$. Therefore, according to SVD theory, the inputs $\psi_{\mathbf{u}_k}$ and outputs $\sigma_k\phi_{\mathbf{v}_k}$ can be uniquely specified at least within phase factors and arbitrariness of degenerate solutions.

The transmission matrix $\mathbf{M_c}$ is, in general, non-unitary, for instance, due to diffraction and scattering in the medium in between as well as finite size and number of apertures; nonetheless, $\mathbf{M_c}$ can always be factorized according to SVD, which means that the orthogonal channels of an optical system do always exist. However, in many practical situations $\mathbf{M_c}$ is not known apriori, so that the modes of the system cannot be calculated.

In [3] we proposed to use a pair of reconfigurable photonic processors to automatically find the best-coupled modes of the system. As shown in Fig. 1, the two photonic processors, noted by $\hat{\mathbf{U}}$ and $\hat{\mathbf{V}}$, are placed at the transmitter and receiver side, respectively, and are configured in a way to estimate the unitary matrices of the system as

$$\hat{\mathbf{V}}^{\dagger}\mathbf{M_c}\hat{\mathbf{U}} = \hat{\mathbf{\Sigma}}. \tag{2}$$

In other words, the two-processor system performs in situ the singular value diagonalization of $\mathbf{M_c}$ which results in obtaining the singular values of the mode pairs (in descending order of coupling strength) at the output. The coupled power using a mode pair of the system is represented by the diagonal terms of $\hat{\mathbf{\Sigma}}$, i.e., $|\sigma_{ij}|^2$, with $i = j$, and the cross-talk between orthogonal modes is evaluated by off-diagonal terms $|\sigma_{ij}|^2$, with $i \neq j$.

b) Realized Device: In our experiment the integrated photonic processors are realized on a standard 220-nm-thick Silicon Photonics platform at AMF foundry. Fig. 2(a) shows a photograph of the realized PIC. The waveguides are 500 nm wide and the PIC is designed for operating in the wavelength range around $\lambda = 1550$ nm. It consists of two MZI diagonals in which each MZI is made of two directional couplers and two thermo-optic phase shifters (inset figure). The input/output couplers for chip-to-free-space coupling and vice versa are grating couplers that are configured in a square array of $100\,\mu$m width. The large spacing ($\gg \lambda/2$) between the array elements leads to multiple diffraction orders in the far field beams, which are denoted by the capital letters, $\Psi_{\mathbf{u}_k}$ and $\Phi_{\mathbf{v}_k}$ (Fig. 1). Each MZI diagonal is configured to generate or sort an orthogonal beam that is coupled through a grating coupler array and is fed to or from the input/output waveguides I/O_1 and I/O_2 of the two-diagonal MZI mesh as shown in Fig. 2(a).

c) Configuration of Photonic Processors: To configure the two processors to generate and receive the mode-pairs of the optical system, light is first injected into the left processor's input waveguide I_1 (Fig. 1). Initially, the first MZI diagonal (color-coded in blue) is in a random state, so some light is coupled out of its array of grating couplers, propagating through the optical system, with some light then arriving at the apertures of the second processor on the right. However, the blue diagonal in the right processor can act as a self-aligning beam coupler [4], i.e., the power coupled at its N apertures (grating couplers) can be coherently summed up to the first output waveguide O_1. This alignment is achieved by sequentially maximizing the output power of each MZI in the diagonal by actuating on the pair of phase shifters [Fig. 2(a)]. Next, light is backward injected into waveguide O_1, which leads to light propagating through optics to arrive the apertures of the left processor and the blue diagonal in the left processor is aligned to maximize the power at I_1. Iterating this forward-and-backward process forms the best-coupled mode pairs of the system [1]. Interestingly, the same best-coupled solutions of the system can also be found exactly by operating in forward-only mode the processors, by exploiting feedback signals from both the transmitter and receiver to maximize the output power at O_1 (see Supplementary material of Ref. [3]).

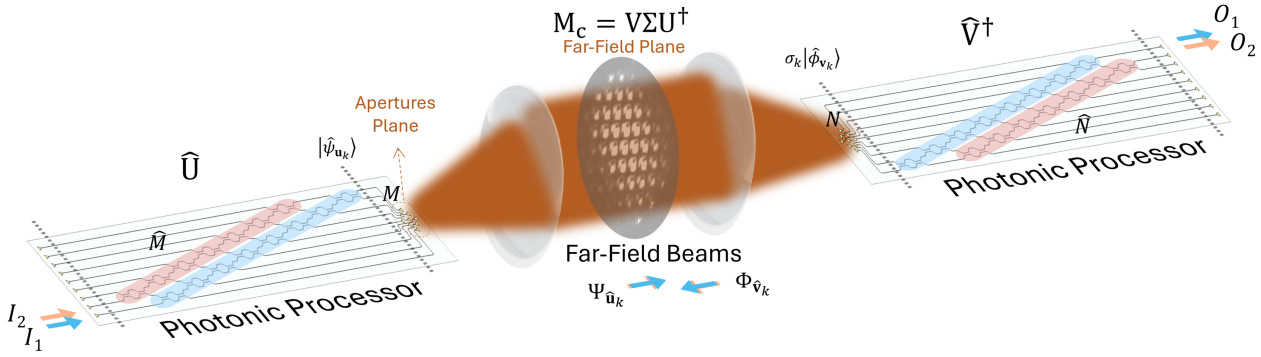

Fig. 1. A pair of photonic processors are placed one at the transmitter side with M optical apertures and one at the receiver side with N apertures to determine automatically the orthogonal communication modes of an arbitrary linear optical system defined by $\mathbf{M_c}$ (from [3]).

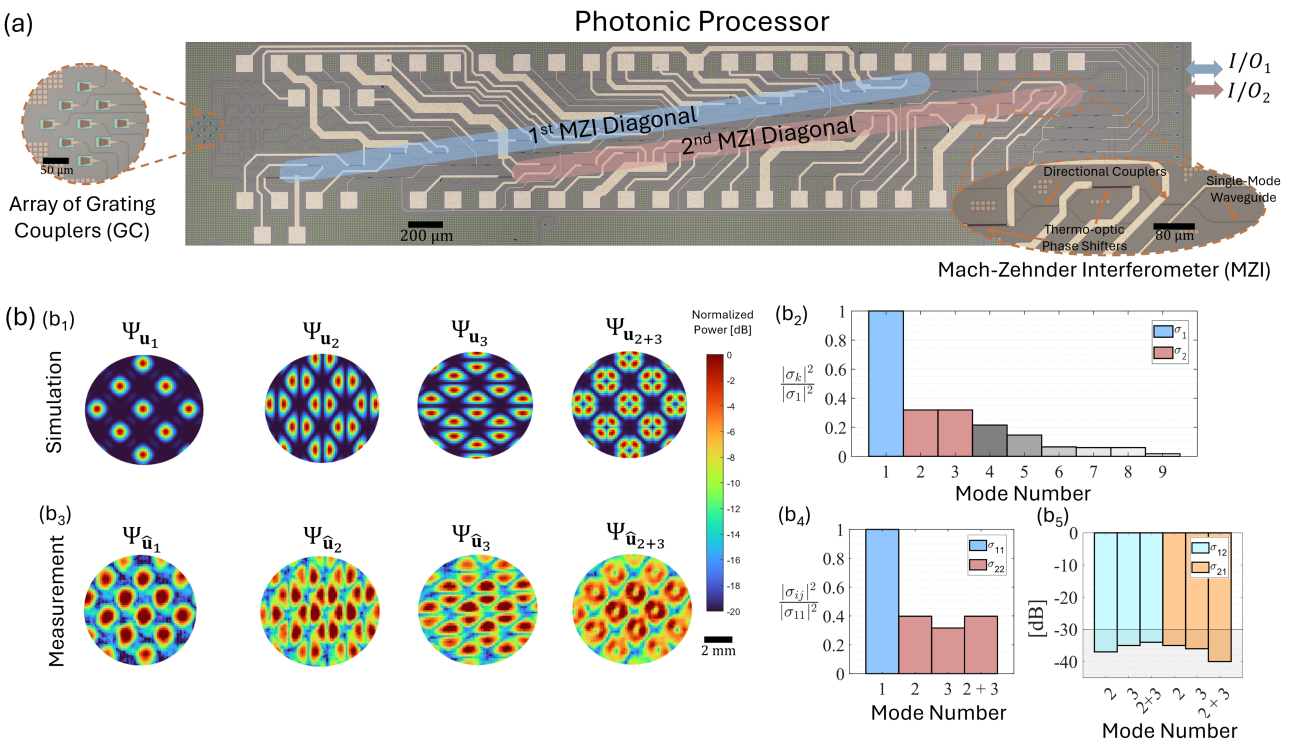

Fig. 2. (a) Silicon photonic PIC realized in a commercial foundry run consisting of a 3×3 array of grating couplers as sampling apertures, connected to a two-diagonal photonic processor with thermally-tuned MZIs. (b) simulation and measurement results of determining the communication modes of the optical system consisting of identical apertures on each side, i.e., $M = N = 9$: (b_1)–(b_2) showing the simulated far-field beam shapes (singular vectors after propagation in far field) and coupling strengths (normalized singular values), and (b_3)–(b_4) showing the measurement results for the first three mode with highest coupling strengths, automatically obtained after configuration of the two processors (from [3]).

Once the blue diagonals are configured to find the first mode, the process is repeated for the pink diagonals to obtain the second mode of the system. The system (here providing the first two modes of the system) can be extended to more modes by adding more diagonals. Once the system converges to its final state, the mode-dependent loss and cross-talk between the two modes are given by the estimated singular-value matrix as

$$\hat{\mathbf{\Sigma}} = \begin{bmatrix} \sigma_{11} & \sigma_{12} \\ \sigma_{21} & \sigma_{22} \end{bmatrix} \tag{3}$$

The squares of these matrix elements can be normalized relative to the power of the first mode, i.e., to $|\sigma_{11}|^2$.

2) Results and Achievements:

a) In-situ optical SVD: Let us consider a system where the two sets of apertures are identical to the 2D array ($M = N = 9$) shown in Fig. 2(a). Fig. 2(b_1) shows the numerical simulation of the singular vectors for the first three modes after free space propagation in the far field, i.e., $\Psi_{\mathbf{u}_k}$, $k = \{1, 2, 3\}$. The end-to-end coupling strengths (or mode-dependent losses) $|\sigma_k|^2$ are given in Fig. 2(b_2) for all 9 possible orthogonal mode pairs (normalized to the coupling strength of the principal mode $|\sigma_1|^2$). Note that some mode numbers, $\{2, 3\}$ and $\{6, 7, 8\}$, share the same coupling strength and form degenerate sets, meaning that a combination of these modes is also acceptable [as shown in Fig. 2(b_1)].

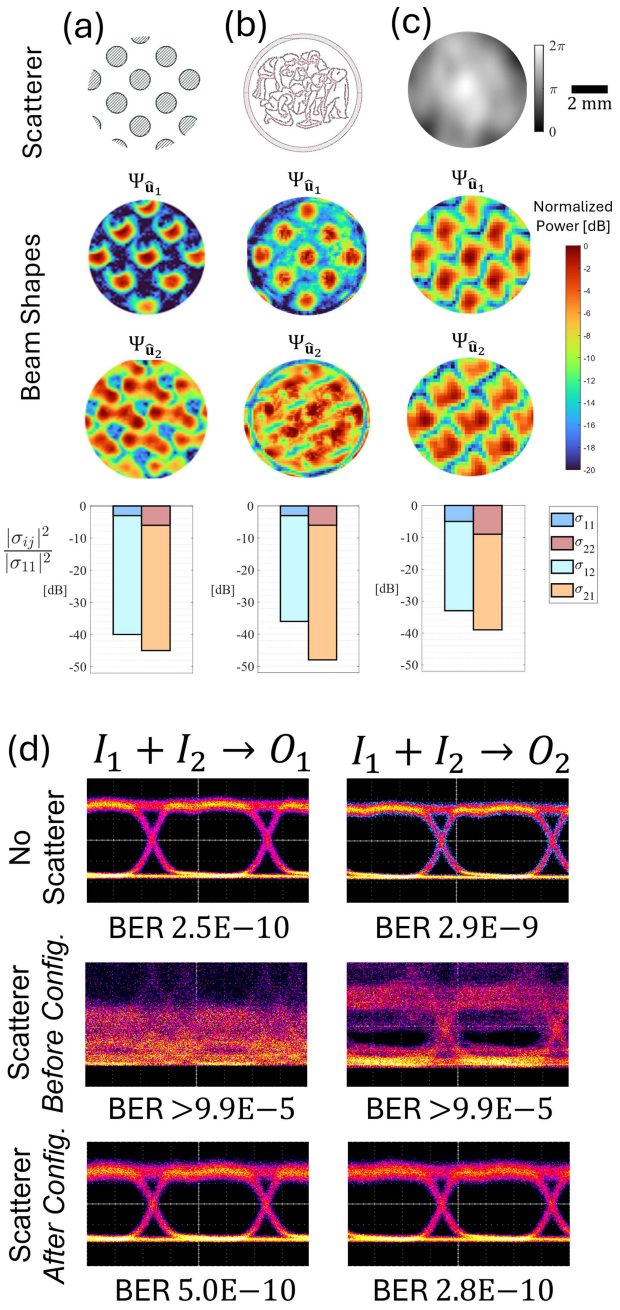

Fig. 3. (a)–(c) Three different obstacles used in the experiments to induce perturbations on the link; first row showing the type of obstacles (left to right: periodic metal obstructions, Politecnico di Milano logo, and phase-only aberration, respectively); middle rows showing the far-field beam shapes of the two modes after reconfiguration of the two processors; bar plots in the last row reporting the coupling strengths and crosstalks after reconfiguration. (d) Results of the transmission experiment done by sending two independent 5 Gbps NRZ-OOK-modulated signals. Initial case (first row), after introducing the scatterer (middle row), and after reconfiguration of the processor (last row) for each of the two established channels (columns) (from [3]).

This result was then confirmed experimentally in an optical setup where two integrated processors are used as in the configuration of Fig. 1. Fig. 2(b$_3$) shows that the shapes of the measured far-field $\Psi_{\hat{\mathbf{u}}_k}, k = \{1, 2, 3\}$ are in good agreement with the simulated ones, as well as the end-to-end normalized coupled power, which is reported in the bar chart of Fig. 2(b$_4$). Notably, these modes exhibit a mutual cross-talk as low as < -30 dB, as shown in Fig. 2(b$_5$), demonstrating that they are indeed the best-coupled orthogonal modes of the system, as provided by the SVD of the transmission matrix $\mathbf{M_c}$ of the system.

b) Modes of scattering systems: Optimal modes can be determined even when unknown scatterers are present in the path between two processors. Scattering can introduce different mode-dependent losses and larger mutual crosstalk, thus making the transmission matrix $\mathbf{M_c}$ strongly non-unitary. Some examples of obstacles that we considered in our experiments are shown in the first row of Fig. 3(a)–(c). If we insert such obstacles in a system configured for a free path without obstacles, the orthogonality between the previously determined modes is broken. However, once we reconfigure the two processors on either sides in the presence of the obstacle, we can compensate partly for the induced losses and obtain again a very low crosstalk between these channels. The far-field beam shapes of the first and second modes that are optimized for the three considered obstacles are in second and third rows of Fig. 3. As reported in the bar charts in the last row of Fig. 3(a)–(c), the mutual cross-talk is less than < -30 dB, meaning that these modes, whose shape does not belong to any conventional family of modes for free-space optical beams, are actually the orthogonal modes of the system for each specific obstacle.

c) Data transmission on orthogonal channels of scattering systems: The establishment of orthogonal communication channels through arbitrary scattering media enables cross-talk-free transmission of parallel data streams without the need of electronic digital signal processing. To this end, we performed data transmission experiments by using two independent 5 Gbps non-return-to-zero (NRZ) on-off-keying (OOK) intensity-modulated signals sharing the same wavelength of 1550 nm. Fig. 3(d) shows the eye diagrams and the bit-error ratio (BER) of the two signals, which are injected at inputs I_1 and I_2 of the processor on the left and are extracted at outputs O_1 and O_2 of the processor on the right. Initially, the system is configured without any scatterer in the free-space path between the two processors and the two data streams are transmitted on the first and second orthogonal modes, respectively. The low cross-talk between the two modes results in open eye diagrams and a very low BER for both signals [first row of Fig. 3(d)]. If we introduce a scatterer in the path, orthogonality between these two modes is broken, and the mutual crosstalk between them significantly deteriorates the quality of the received signals (middle row). However, as we configure again the two processors, a new pair of low-cross-talk orthogonal modes is found automatically, with eye diagrams and BER performance (last row) similar to the reference ones observed in the absence of the scatterer (first row).

B. Related Works on Mode Manipulation Using Integrated Photonic Processors

Reconfigurable PICs have been recently used in several works for manipulating fiber or free-space modes. Here, we briefly summarize the proposed approaches based on integrated photonic processors, along with the most relevant demonstrations achieved as of 2024.

1) Fiber Modes: Photonic integrated circuits can be used to selectively couple and (de)multiplex fixed modes of a few-mode fiber (FMF) [4], [5], [6], [7], [8], [9], [10], [11], [12], [13], [14], [15]. Typically, the coupling of the optical fiber to the single-mode waveguides of the photonic chip is done in two ways: i) by sampling the fiber field using couplers typically implemented via single- or dual-polarization grating couplers, whose arrangement onto the chip is optimized according to the shape of the modes to be extracted [4], [6], [7], [10]; ii) via specifically designed multi-mode structures based on the mode of the custom-designed multi-mode fiber [5], [13]. Selected modes can then be routed to the output one at a time or can be mapped to specific outputs by a simple passive structure [14], [15].

The extension to reconfigurable multiple mode extraction and sorting can be done using integrated photonic processors [4]. The PIC for multi-mode unscrambling normally consists of two parts: first, as in previous examples, a multi-aperture or multi-mode input coupler is required to map 2D polarized mode into a 1D array of single-mode waveguides, while preserving the orthogonality between the modes (unitary transformation); second, a unitary processor, such as a triangular MZI mesh processor, is employed to route coupled orthogonal (super-)modes in the input waveguides to different output waveguides. A recent demonstration of this approach is reported in the work by Lu et al. [11], in which they demonstrated de-scrambling of 6 polarization and transverse modes of an FMF [Fig. 4(a)]. In their work the coupling structure is a 2D multi-mode grating coupler connected at 4 ports to asymmetric directional couplers to route different coupled portions of the fiber modes to different single-mode waveguides. These contributions are then sorted out on different output waveguides using an 8×8 MZI-based triangular photonic processor, which has the same architecture as in our work [3]. A low cross-talk level (< 21 dB) is demonstrated in the presence of three concurrent data-modulated signals at 32 Gbps.

In another work by Yi and coworkers [16], a photonic integrated processor is used in an FMF communication system as an adaptive multi-mode receiver; the processor effectively separates two different spatial channels or two different polarization of the same spatial channel with unknown mixing/crosstalk introduced during fiber transmission.

2) Free-Space Modes: In the case of free space, beam manipulation with PICs was initially investigated mainly to perform beam steering operations for applications such as light detection and ranging (LiDAR) [19], [20], [21], [22], [23], [24]. Multiple free-space couplers (apertures), typically grating couplers in a 1D or 2D array configuration, are integrated on the photonic chip to build an optical phased array with a large emitting aperture; the direction of the low-divergence Gaussian-shaped beam is controlled through an array of integrated phase shifters within the field of view of the elementary aperture and propagates from the chip towards the object to be ranged or detected. Recent steering approaches based on focal-plane arrays (using external lenses) have also been proposed [22], [23].

However, multi-port reconfigurable PICs offer the possibility of controlling more degrees of freedom of free-space beams,

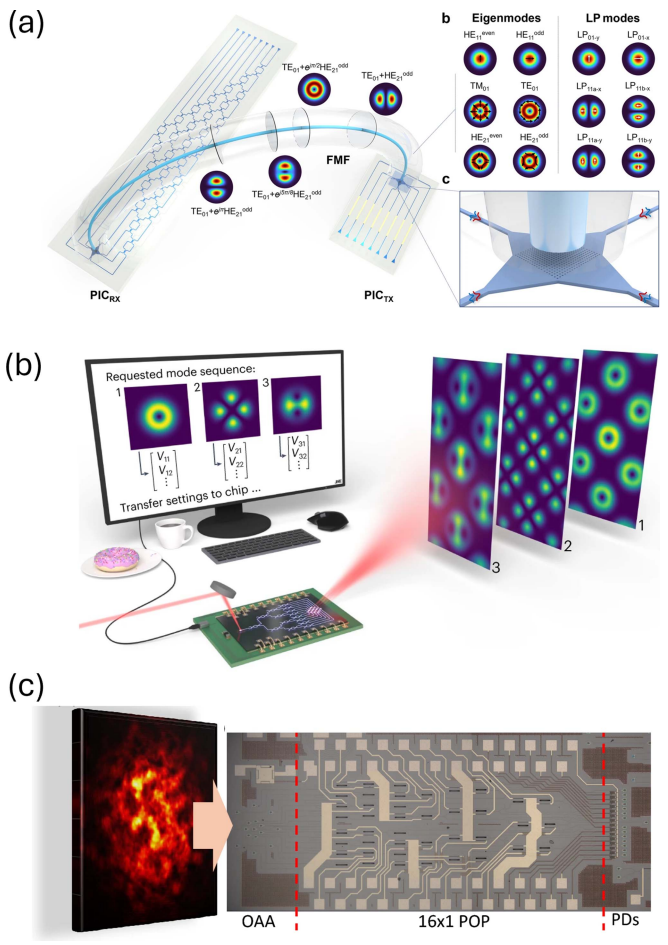

Fig. 4. Examples of arbitrary-mode manipulation enabled by PICs. The circuits typically consists of a coupler structure (array of sampling apertures or specifically-designed component) connected to a reconfigurable MZI-based photonic processor. Application examples are for (a) demultiplexing modes of an FMF (from [11]) (b) generating arbitrary free-space beams (from [17]), and (c) receiving and coupling a perturbed beam to the chip (from [18]).

thus enabling the generation, manipulation and detection of arbitrary-shaped multi-mode beams. For example, a 16-element 2D optical phased array controlled by thermal phase shifters was used to generate and sort OAM beams for free space coherent optical communication [25]. Other approaches based on phased arrays were proposed to generate OAM or Bessel beams [26], [27]. Song et al. demonstrated a 10-Gbit/s free-space communication link using an LG beam with tunable radial and azimuthal modal indices generated by a circular antenna array controlled by a reconfigurable PIC [28].

For transmission through arbitrary scattering media that causes (unitary or non-unitary) mode mixing, independent control of both amplitude and phase of the electric field emitted (or received) by the on-chip apertures is necessary [81]. An example of such functionality is reported in [29], where a photonic processor is used to couple an arbitrary beam into the chip and to spatially resolve such multi-mode beams. More recently, Butow et al. [17] used a similar PIC architecture to generate free-space structured beams [Fig. 4(b)]. In this case the free-space apertures are composed of a 2D array of focusing grating couplers (similar

to our work [3]), and the MZI-based photonic processor has a 16×1 binary-tree architecture. The presented approach allows the generation and control of free-space structured light, such as high-order Hermite–Gaussian and Laguerre–Gaussian beams and their combinations, on demand and in real time.

The same architecture based on a binary-tree MZI mesh processor connected to a 2D array of grating couplers has been used by Martinez et al. to demonstrate adaptive mitigation of beam scintillation caused by free-space propagation in a turbulent environment [18]. In this work [see Fig. 4(c)], the PIC is used as an FSO receiver to couple a data-modulated OOK signal at 10 Gbps after propagation in an atmospheric turbulence emulator. The adaptive photonic chip provides a significant reduction of the intensity fading at the receiver and offers an efficient solution for the coupling of turbulent FSO beams to single-mode optics. Compared to digital signal processing approaches, turbulence mitigation in the optical domain using an analog photonic processor offers energy-efficient and cost-effective operation, along with modulation format and data rate independence, and compatibility with commercial fiber optic transceivers.

C. Mode Manipulation Technologies

Space diversity and space division multiplexing (SDM) are well-established concepts in communications systems, such as in MIMO wireless systems, to implement high-capacity microwave links. In the optical domain, as well, static and reconfigurable photonic devices have been extensively used for the manipulation of optical modes in SDM communications. Here, we briefly summarize these approaches realized in different technologies, namely photonic lanterns, multi-plane light converters, and integrated photonics.

1) Photonic Lanterns: Space multiplexing has been known for several decades for fibers [30]; however, only recently it has started to be seriously considered as a strategy to face the capacity crunch of optical fibers [31]. These typically exploit multi-core or FMF to perform SDM, and for demultiplexing the modes, digital signal processing (DSP) is needed to undo possible mixing in the signals due to propagation in the fiber. The digital processors, which need to run at the bit rate of the optical signal, are modulation format and protocol dependent, and as the data rate increases, do not offer a scalable approach in terms of power consumption and time latency. Therefore, several different solutions, passive or reconfigurable, have been proposed to perform all-optical demultiplexing of such modes.

Fig. 5(a) shows the existing approaches based on photonic lantern technology. One solution uses 3-dimensional (3D) fiber structures that convert the modes from FMFs to single-mode fibers or a fiber bundle [panel a_1]. They require a suitable design of the fiber core and cladding dimensions and spacing to adiabatically convert higher-order modes while keeping low inter-modal cross-talk [32], [33], [34]. There exist also approaches based on fiber directional couplers to selectively excite the modes of an FMF [35].

Similar devices can be fabricated using laser-inscribed 3D waveguides [panel a_2]. These integrated devices were first used

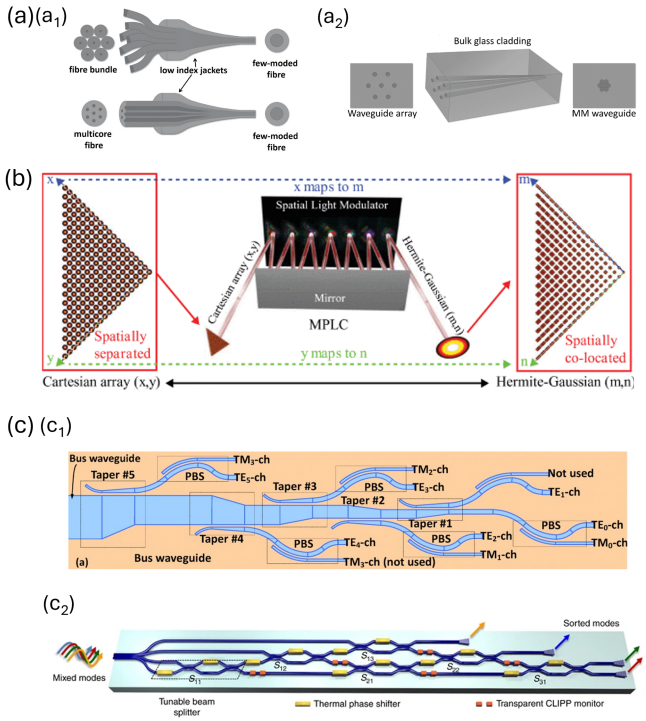

Fig. 5. Existing mode manipulation technologies, (a) using 3D structures such as (a_1) photonic lanterns and (a_2) glass waveguides (from [34]), (b) MPLC technology consisting of discrete phase plates for successive phase manipulation (from [42]), and (c) integrated photonics for (c_1) static or (c_2) reconfigurable mode (de)multiplexing in planar waveguides (from [49], [50], respectively).

for astronomical applications and mainly for 2D-to-1D mapping [36]; however, similar to their fiber optics counterpart, they can be dimensioned to perform mode demultiplexing of FMFs [37].

2) Multi-Plane Light Conversion: Free-space bulk optical devices can also be used to perform spatial (de)multiplexing. The simplest approach consists of generating fixed modes using a number of discrete phase masks and then combining the transformed beams via beam combiners [38], [39]; however, due to the bulkiness of the discrete elements, the intrinisic losses of beam combiners, and alignment issues this approach is not easily scalable to a large number of modes. A more compact solution exploits a multi-plane light converter (MPLC), which is made of a set of phase masks followed by free-space propagation to convert a whole set of beams (for instance spatially-separated Gaussian beams) to another set of orthogonal beams [40], [41], [42]. As shown in the example of Fig. 5(b), an MPLC performs 2D refractive index (and therefore phase) transformations along with an optical Fourier transform (propagation in a folded path here, or via lenses) to implement a lossless (unitary) transformation between input and output mode sets. MPLCs can handle multiple modes with low crosstalk and high accuracy and can be seen as a discrete counterpart of the transformation performed using photonic lanterns. To address individual modes the number of required phase masks is, in general, equal to the number of modes; however, conversion between specific sets of fixed modes may require a much smaller

number of phase transformations [42], [43]. MPLCs performing transformations of a large number of modes have been demonstrated (> 200) [42]; however, these devices can only convert predefined sets of fixed modes without any reconfigurability.

To add reconfigurability to MPLC-based schemes, the phase masks can be realized using Spatial Light Modulators (SLM) [44], [45], [46]. SLMs can provide arbitrary programmable 2D phase profiles and can in principle be used to generate and convert arbitrary mode shapes; however, apart from bulkiness, cost, and phase-only manipulation of the beams, they may induce losses due to the presence of higher diffraction orders or scattering at the pixels. Their refresh rate for adapting to time-varying scenarios is reported to be maximum of the order of few kHz for commercial devices today [47], [48]

3) Integrated Photonics: As presented in previous section with a number of recent examples, integrated photonic technology enables mode manipulation for both free-space and guided modes. The manipulation approaches using waveguides share similarities with technologies mentioned above [51]. For instance, asymmetric directional couplers (ADCs) are extensively used as static (de)multiplexers of waveguide modes as they realize mode mapping between high-order modes of multimode waveguides and the fundamental mode of single-mode waveguides with simple and compact structures. In these structures, mode-selective coupling is achieved by phase-matching the modes to be coupled through a suitable waveguide tapering (similar to photonic lanterns), as shown in the example of Fig. 5(c_1) [15], [52]. More compact broadband devices to realize on-chip mode (de)multiplexers have also been proposed that exploit sub-wavelength structures that are optimized using inverse design methods [53], [54] and can also achieve a broad wavelength range of operation.

A reconfigurability degree can be added to such multi-mode multiplexers, for example, to realize multi-mode switches or add/drop multiplexers [55], [56], [57], [58]. This also enables multidimensional multiplexing that exploits mode along with wavelength multiplexing, for instance, to scale up the number of optical communication channels [59], [60], [61]. To realize a fully reconfigurable on-chip mode multiplexer that can sort out arbitrary input guided modes, an approach based on successive phase manipulation (similar to the MPLC using phase plates) is proposed [50]. Using layers of tuneable beam combiners [panel c_2], implemented by MZI diagonals as in the photonic processors in previous sections, the field components of each input mixed mode are coherently summed and sorted out arbitrarily at different single-mode output waveguides.

III. Discussions and Perspectives

Reconfigurable PICs provide scalable and reliable technology for implementing advanced manipulation of the modes of various systems. The solutions discussed in Secs II-B and II-C generally work well for a subset of known fixed modes of fibers, waveguides and free-space, and their scalability and adaptation for arbitrary high-order and time-varying modes of realistic environments would be challenging. With respect to previous work, our approach has the advantage of handling arbitrary modes and can extend mode manipulation schemes to systems that vary in time in an unpredictable way or complex optical systems in which the communication modes are unknown and cannot be calculated a priori.

In the following we discuss the main challenges to the practical implementation of mode manipulation using the proposed PIC-based approach and the impact that this technology could have in different fields of applications.

A. Limitations

The main limitations to the scaling and performance of reconfigurable PICs for mode manpulation are here identified and discussed. The étendue principle [62] (or, equivalently, the general impossibility of combining two mutually incoherent modes losslessly into one) is the only thermodynamic limit to be considered; the other limits are mainly technological limits that will be relieved with the progress of the platforms.

- *Optical coupling:* Free-space-to-chip coupling is done by making use of grating couplers which induce limitations in terms of loss and size when forming an array. Also, their emission angle and efficiency dependency on the wavelength may cause issues for point-to-point free-space communication links. Lenslet arrays on top of the grating couplers can improve light collection but at the cost of reducing the field-of-view (étendue property). The top emission efficiency can be increased, for example, by having non-symmetric multiple-layer designs [63], [64], [65], [66]. Other coupling solutions can be adopted, such as photonic lanterns or MPLC technologies in combination with edge couplers on the chip for coupling low-order free-space modes, though at the cost of increasing packaging complexity and losses.
- *Phase actuators:* The phase shifters implemented in an MZI building block as a tuneable beam combiner are conventionally based on the thermo-optic effect. This has implications in terms of electrical power consumption and increasing thermal cross-talk on the chip for scaling up the number of available modes. Other types of phase shifters such as p-n junction or micro-electro-mechanical actuators are available and are compatible with the SiPh platform. Other approaches that have attracted the interest of researchers include heterogeneously integrated electro-optic materials (e.g., thin-film lithium niobate, TFLNO [67], [68] or barium titanate, BTO) [69], [70], [71]), phase change materials (PCM) [72], [73], or micro-electromechanical switches (MEMS) [74]; however, at the moment each suffers from different issues, such as induced losses, size, high-drive voltage, etc.
- *Control electronics and footprint:* The electronics for controlling the phase shifters and reading out the light monitors in the MZI block cell need to work according to the configuration speed needed to adapt to the application scenario (e.g., in the range of kHz for atmospheric turbulence compensation). Considering the scalability, the

number of input/output electrical pads needed for the actuators or read-out and the routing of the metal layers induce limitations on the footprint. Moreover, the reduction of parasitic effects and noise, and the high sensitivity required by high quality electronic control layers, motivate a monolithically integrated platform in which photonic and electronic circuits share the same chip [75], [76]. For relatively low-speed applications (with respect to the actuator speed), monolithically integrated electronics to perform time-multiplexing on actuating and read out electrical signals could be a solution to overcome this issue [77], [78].

The photonic processor is typically based on MZIs in a binary-tree or triangular (or reduced to multiple diagonals) configuration to perform a simple and fast self-configuring algorithm; however, these architectures are longer than, for instance, rectangular architectures in terms of footprint [79], [80].

- *Mode scalability:* The maximum number of spatial channels that can be efficiently multiplexed and transmitted through an arbitrary system -corresponding to the number of effective modes- is determined by the non-zero singular values of the coupling matrix $\mathbf{M_c}$ [3]. For a system comprising M transmitting apertures and N receiving apertures, this number is fundamentally limited by $\min(M, N)$. The introduction of additional apertures on both ends of the system can potentially enable additional transmission channels. However, the actual number of non-zero singular values is influenced by the transmission medium in between the two processors, and, as illustrated in Fig. 2(b_2), higher-order modes may exhibit significantly lower singular values. Increasing the number of optical apertures can enhance the coupling strength of the modes [3]. In terms of circuit complexity, the number of MZIs required per processor scales quadratically with the number of channels. Specifically, in a symmetric system with $M = N$ apertures, a total of $M(M-1)/2$ MZIs per processor is necessary to fully establish all the available modes [4]. In principle, provided that the two processors are appropriately configured, the crosstalk between all channels remains unaffected as more channels are simultaneously utilized.

B. Impact and Future Vision

Apart from the great potential foreseen in the area of communications, the achievements discussed in this paper can be considered a breakthrough as they can have a large impact in many different fields, such as:

- *Optical Communications:* In SDM, where the modes of multimode or few-more fibers are used as separate channels to transmit multiple data streams concurrently, our approach can be used to customize mode profiles for optimal performance. For instance, it can be used to select the best modes that optimize communications depending on fiber conditions and facilitate efficient (de)multiplexing with minimum crosstalk. Notably, the architecture supports multi-dimensional data transmission schemes, including coherent, wavelength, and polarization diversity, in conjunction with SDM to further expand communication capacity. The flexibility of the architecture also supports free-space SDM, where sampling apertures can enable effective free-space-to-chip coupling and the use of arbitrary modes can help mitigate atmospheric distortions on the wavefront, as the system can dynamically adapt the modes based on environmental conditions [18], [81].
- *Optical Sensing:* In multimode fibers, different modes exhibit different sensitivities to external factors such as temperature, pressure, and strain [82]. Monitoring the modal properties such as phase, intensity and polarization of customized modes (which are selected to maximize their sensitivity to different parameters) would enable the implementation of distributed multi-parametric sensors for environmental and structural monitoring [83]. In free space, the decomposition of optical beams in arbitrary modes can be used to analyze complex wavefronts [29], providing insights into atmospheric turbulence or beam distortions, and for separation and measurement of partially coherent light [84]. Potential applications in astronomical sensing are also now being explored [85].
- *Beam Shaping and Steering:* Selective excitation and combination of modes with specific beam profiles would provide additional degrees of freedom for shaping the light beams [17], [86]. In LiDAR systems, exploiting combinations of higher-order modes could enhance detection accuracy and resolution for object recognition and distance measurement, providing additional spatial information about targets.
- *Imaging and Microscopy:* Advanced manipulation of high-order optical modes would enable imaging and microscopy to further enhance resolution, contrast, and functionality beyond what is achievable with standard Gaussian beams or low-order modes. Structured illumination patterns, with optimal amplitude, phase and polarization profile, can be generated, which interact with the sample's spatial frequency content, enabling super-resolution imaging by recovering information beyond the diffraction limitation, reducing background noise and improving visibility of fine structures [87].
- *Quantum Communication and Computing:* As in classical optical communications, different modes can be used to carry independent quantum channels and increase the capacity of quantum communication systems [88]. Encoding qubits in the optimal modes of a system would improve the fidelity of quantum key distribution over free-space or fiber-optic links, by increasing the resilience against atmospheric turbulence or other noise sources, while enhancing key transmission rates [89]. In photonic quantum computing, the manipulation of arbitrarily shaped beams would provide additional degrees to realize high-dimensional logic gates and to generate spatially structured light beams for the photonic control of quantum system (trapping of ions and neutral atoms) [90].

- *Photonic computing:* A further possible application is in photonic computing, semantic communication, and information extraction. Mathematically, such photonic processors implement arbitrary linear operators (unitary and non-unitary), which can be described by sums and multiplications. This means that operations such as matrix vector multiplications (MVMs), matrix-matrix multiplications (MMMs), multiplication and accumulation (MAC), convolutions and cross-correlations, linear transformations (Fourier, Hilbert, Hadamard, etc.) can be efficiently operated in the optical domain. For this reason, photonic computing is of strategic impact in emerging applications requiring massive data processing, like artificial intelligence (AI) and machine learning (ML). In neural networks, $> 80\%$ of the processing time and energy cost is associated to such linear operations and data transfer among computational units [91], whose weight scales quadratically with the size of the dataset to be processed. Replacing (and/or complementing) electronic DSP with photonic hardware accelerators and photonic interconnects is expected to boost the scalability of AI systems, by increasing the computational power, reducing the latency, and reducing energy consumption and carbon footprint.

IV. Conclusion

The breakthrough presented in this paper highlights a transformative approach to leveraging the degrees of freedom offered by optical modes, which are still substantially unexploited. Unlike previous works in the field, where mode manipulation in both free-space and guided optics was constrained to fixed or predetermined modes of specific systems, our approach removes this limitation. We extend the concept of mode manipulation to arbitrary modes of arbitrary systems. We demonstrated that, by employing reconfigurable PICs, it is possible to dynamically identify in-situ the optimal communication modes through complex, time-varying, and even unknown media, without requiring prior knowledge or calibration of the system. These modes may not belong to any conventional mode families typically used in optics. However, they represent the true communication modes of the system, ensuring maximum end-to-end power transmission and mutual orthogonality. Additionally, we reviewed related works from other groups that demonstrate the versatility of reconfigurable PICs in generating free-space structured beams, advanced amplitude/phase detection of wavefronts, and correcting dynamically distorted beams.

These findings confirm the potential of reconfigurable PICs to significantly extend existing schemes for mode manipulation, addressing more complex and realistic scenarios. This advancement holds many implications across diverse fields, including integrated sensing and communication systems, hyper-resolution imaging and microscopy, precision metrology and ranging, quantum communication, and photonic computing.

References

[1] D. A. B. Miller, "Establishing optimal wave communication channels automatically," *J. Lightw. Technol.*, vol. 31, no. 24, pp. 3987–3994, Dec. 2013. [Online]. Available: https://ieeexplore.ieee.org/document/6581883

[2] D. A. B. Miller, "Waves, modes, communications, and optics: A tutorial," *Adv. Opt. Photon.*, vol. 11, no. 3, pp. 679–825, 2019. [Online]. Available: https://opg.optica.org/abstract.cfm?URI=aop-11-3-679

[3] S. SeyedinNavadeh et al., "Determining the optimal communication channels of arbitrary optical systems using integrated photonic processors," *Nature Photon.*, vol. 18, no. 2, pp. 149–155, 2024. [Online]. Available: https://www.nature.com/articles/s41566-023-01330-w

[4] D. A. B. Miller, "Self-aligning universal beam coupler," *Opt. Exp.*, vol. 21, no. 5, pp. 6360–6370, 2013. [Online]. Available: https://opg.optica.org/abstract.cfm?URI=oe-21-5-6360

[5] C. R. Doerr, N. K. Fontaine, M. Hirano, T. Sasaki, L. L. Buhl, and P. J. Winzer, "Silicon photonic integrated circuit for coupling to a ring-core multimode fiber for space-division multiplexing," in *Proc. 37th Eur. Conf. Exhib. Opt. Commun.*, 2011, pp. 1–3, ISSN: 1550-381X. [Online]. Available: https://ieeexplore.ieee.org/document/6065926?arnumber=6065926

[6] N. K. Fontaine et al., "Space-division multiplexing and all-optical MIMO demultiplexing using a photonic integrated circuit," in *Proc. OFC/NFOEC*, 2012, pp. 1–3. [Online]. Available: https://ieeexplore.ieee.org/abstract/document/6192240

[7] A. M. J. Koonen, H. Chen, H. P. A. van den Boom, and O. Raz, "Silicon photonic integrated mode multiplexer and demultiplexer," *IEEE Photon. Technol. Lett.*, vol. 24, no. 21, pp. 1961–1964, Nov. 2012. [Online]. Available: https://ieeexplore.ieee.org/document/6304909

[8] D. Melati, A. Alippi, and A. Melloni, "Reconfigurable photonic integrated mode (de)multiplexer for SDM fiber transmission," *Opt. Exp.*, vol. 24, no. 12, pp. 12625–12634, 2016. [Online]. Available: https://opg.optica.org/oe/abstract.cfm?uri=oe-24-12-12625

[9] B. Wohlfeil, G. Rademacher, C. Stamatiadis, K. Voigt, L. Zimmermann, and K. Petermann, "A two-dimensional fiber grating coupler on SOI for mode division multiplexing," *IEEE Photon. Technol. Lett.*, vol. 28, no. 11, pp. 1241–1244, Jun. 2016. [Online]. Available: https://ieeexplore.ieee.org/document/7372392/?arnumber=7372392

[10] T. Watanabe, "Coherent few mode demultiplexer realized as a 2D grating coupler array in silicon," *Opt. Exp.*, vol. 28, no. 24, pp. 36009–36019, 2020. [Online]. Available: https://doi.org/10.1364/OE.406251

[11] K. Lu et al., "Empowering high-dimensional optical fiber communications with integrated photonic processors," *Nature Commun.*, vol. 15, no. 1, 2024, Art. no. 3515. [Online]. Available: https://www.nature.com/articles/s41467-024-47907-z

[12] W. Zhou et al., "Efficient and adaptive reconfiguration of light structure in optical fibers with programmable silicon photonics," 2024. [Online]. Available: http://arxiv.org/abs/2410.15172

[13] K. Y. Yang et al., "Multi-dimensional data transmission using inverse-designed silicon photonics and microcombs," *Nature Commun.*, vol. 13, no. 1, 2022, Art. no. 7862. [Online]. Available: https://www.nature.com/articles/s41467-022-35446-4

[14] C. R. Doerr, "Proposed architecture for MIMO optical demultiplexing using photonic integration," *IEEE Photon. Technol. Lett.*, vol. 23, no. 21, pp. 1573–1575, Nov. 2011. [Online]. Available: https://doi.org/10.1109/LPT.2011.2164061

[15] X. Yi, W. Zhao, L. Zhang, Y. Shi, and D. Dai, "Efficient mode coupling/(de)multiplexing between a few-mode fiber and a silicon photonic chip," *Photon. Res.*, vol. 12, no. 12, pp. 2784–2793, Dec. 2024. [Online]. Available: https://opg.optica.org/prj/abstract.cfm?URI=prj-12-12-2784

[16] D. Yi, Y. Tong, and H. K. Tsang, "Unmixing data lanes in mode-division multiplexing optical fiber transmission using an integrated photonic processor," *J. Lightw. Technol.*, vol. 42, no. 1, pp. 287–292, Jan. 2024. [Online]. Available: https://ieeexplore.ieee.org/document/10243097/?arnumber=10243097

[17] J. Bütow, J. S. Eismann, V. Sharma, D. Brandmüller, and P. Banzer, "Generating free-space structured light with programmable integrated photonics," *Nature Photon.*, vol. 18, no. 3, pp. 243–249, 2024. [Online]. Available: https://www.nature.com/articles/s41566-023-01354-2

[18] A. I. Martinez et al., "Self-adaptive integrated photonic receiver for turbulence compensation in free space optical links," *Sci. Rep.*, vol. 14, no. 1, 2024, Art. no. 20178. [Online]. Available: https://www.nature.com/articles/s41598-024-70726-7

[19] J. Sun, E. Timurdogan, A. Yaacobi, E. S. Hosseini, and M. R. Watts, "Large-scale nanophotonic phased array," *Nature*, vol. 493, no. 7431, pp. 195–199, 2013. [Online]. Available: https://www.nature.com/articles/nature11727

[20] M. J. R. Heck, "Highly integrated optical phased arrays: Photonic integrated circuits for optical beam shaping and beam steering," *Nanophotonics*, vol. 6, no. 1, pp. 93–107, 2017. [Online]. Available: https://www.degruyter.com/document/doi/10.1515/nanoph-2015-0152/html

[21] S. A. Miller et al., "Large-scale optical phased array using a low-power multi-pass silicon photonic platform," *Optica*, vol. 7, no. 1, pp. 3–6, 2020. [Online]. Available: https://opg.optica.org/optica/abstract.cfm?uri=optica-7-1-3

[22] C. Rogers et al., "A universal 3D imaging sensor on a silicon photonics platform," *Nature*, vol. 590, no. 7845, pp. 256–261, 2021. [Online]. Available: https://www.nature.com/articles/s41586-021-03259-y

[23] X. Zhang, K. Kwon, J. Henriksson, J. Luo, and M. C. Wu, "A large-scale microelectromechanical-systems-based silicon photonics LiDAR," *Nature*, vol. 603, no. 7900, pp. 253–258, 2022. [Online]. Available: https://www.nature.com/articles/s41586-022-04415-8

[24] R. Fatemi, A. Khachaturian, and A. Hajimiri, "A nonuniform sparse 2 d large FOV optical phased array with a low power PWM drive," *IEEE J.Solid State Circuits*, vol. 54, no. 5, pp. 1200–1215, May 2019, doi: 10.1109/JSSC.2019.2896767.

[25] T. Su et al., "Demonstration of free space coherent optical communication using integrated silicon photonic orbital angular momentum devices," *Opt. Exp.*, vol. 20, no. 9, pp. 9396–9402, 2012. [Online]. Available: https://opg.optica.org/oe/abstract.cfm?uri=oe-20-9-9396

[26] J. Sun, M. Moresco, G. Leake, D. Coolbaugh, and M. R. Watts, "Generating and identifying optical orbital angular momentum with silicon photonic circuits," *Opt. Lett.*, vol. 39, no. 20, pp. 5977–5980, 2014. [Online]. Available: https://opg.optica.org/ol/abstract.cfm?uri=ol-39-20-5977

[27] J. Notaros, C. V. Poulton, M. J. Byrd, M. Raval, and M. R. Watts, "Integrated optical phased arrays for quasi-bessel-beam generation," *Opt. Lett.*, vol. 42, no. 17, pp. 3510–3513, 2017. [Online]. Available: https://opg.optica.org/ol/abstract.cfm?uri=ol-42-17-3510

[28] H. Song et al., "Free-space optical communication link using a single Laguerre-Gaussian beam with tunable radial and azimuthal spatial indices generated by an integrated concentric circular antenna array," *Opt. Exp.*, vol. 32, no. 19, pp. 33803–33810, Sep. 2024. [Online]. Available: https://opg.optica.org/oe/abstract.cfm?URI=oe-32-19-33803

[29] J. Bütow et al., "Spatially resolving amplitude and phase of light with a reconfigurable photonic integrated circuit," *Optica*, vol. 9, no. 8, 2022, pp. 939–946. [Online]. Available: https://opg.optica.org/abstract.cfm?URI=optica-9-8-939

[30] S. Berdagu and P. Facq, "Mode division multiplexing in optical fibers," *Appl. Opt.*, vol. 21, no. 11, pp. 1950–1955, 1982, doi: 10.1364/AO.21.001950.

[31] D. Richardson, J. Fini, and L. Nelson, "Space-division multiplexing in optical fibres," *Nature Photon*, vol. 7, no. 5, pp. 354–362, 2013 [Online]. Available: https://doi.org/10.1038/nphoton.2013.94

[32] S. G. Leon-Saval, T. A. Birks, J. Bland-Hawthorn, and M. Englund, "Multimode fiber devices with single-mode performance," *Opt. Lett.*, vol. 30, no. 19, pp. 2545–2547, 2005. [Online]. Available: https://opg.optica.org/abstract.cfm?URI=ol-30-19-2545

[33] S. G. Leon-Saval, A. Argyros, and J. Bland-Hawthorn, "Photonic lanterns," *Nanophotonics*, vol. 2, no. 5, pp. 429–440, 2013.

[34] N. K. Fontaine et al., "Photonic lanterns, 3-D waveguides, multiplane light conversion, and other components that enable space-division multiplexing," *Proc. IEEE*, vol. 110, no. 11, pp. 1821–1834, Nov. 2022. [Online]. Available: https://ieeexplore.ieee.org/document/9916270/?arnumber=9916270&tag=1

[35] S. H. Chang et al., "Mode division multiplexed optical transmission enabled by all fiber mode multiplexer," *Opt. Exp.*, vol. 22, no. 12, pp. 14229–14236, 2014. [Online]. Available: https://opg.optica.org/oe/abstract.cfm?uri=oe-22-12-14229

[36] R. R. Thomson, T. A. Birks, S. G. Leon-Saval, A. K. Kar, and J. Bland-Hawthorn, "Ultrafast laser inscription of an integrated photonic lantern," *Opt. Exp.*, vol. 19, no. 6, pp. 5698–5705, 2011. [Online]. Available: https://opg.optica.org/abstract.cfm?URI=oe-19-6-5698

[37] N. Riesen, S. Gross, J. D. Love, Y. Sasaki, and M. J. Withford, "Monolithic mode-selective *few-mode* multicore fiber multiplexers," *Sci. Rep.*, vol. 7, no. 1, 2017, Art. no. 6971. [Online]. Available: https://www.nature.com/articles/s41598-017-06561-w

[38] S. Randel et al., "6 x 56-Gb/s mode-division multiplexed transmission over 33-km few-mode fiber enabled by 6 x 6 MIMO equalization," *Opt. Exp.*, vol. 19, no. 17, pp. 16697–16707, 2011. [Online]. Available: https://opg.optica.org/oe/abstract.cfm?uri=oe-19-17-16697

[39] R. Ryf et al., "Mode-division multiplexing over 96 km of few-mode fiber using coherent 6 x 6 MIMO processing," *J. Lightw. Technol.*, vol. 30, no. 4, pp. 521–531, Feb. 2012. [Online]. Available: https://ieeexplore.ieee.org/document/6074912/?arnumber=6074912

[40] J.-F. o. Morizur et al., "Programmable unitary spatial mode manipulation," *J. Opt. Soc. America A*, vol. 27, no. 11, pp. 2524–2531, 2010. [Online]. Available: https://opg.optica.org/josaa/abstract.cfm?uri=josaa-27-11-2524

[41] G. Labroille, B. Denolle, P. Jian, P. Genevaux, N. Treps, and J.-F. Morizur, "Efficient and mode selective spatial mode multiplexer based on multi-plane light conversion," *Opt. Exp.*, vol. 22, no. 13, pp. 15599–15607, 2014. [Online]. Available: https://doi.org/10.1364/OE.22.015599

[42] N. K. Fontaine, R. Ryf, H. Chen, D. T. Neilson, K. Kim, and J. Carpenter, "Laguerre-Gaussian mode sorter," *Nature Commun.*, vol. 10, no. 1, 2019, Art. no. 1865. [Online]. Available: https://www.nature.com/articles/s41467-019-09840-4

[43] S. Bade et al., "Fabrication and characterization of a mode-selective 45-mode spatial multiplexer based on multi-plane light conversion," *Opt. Fiber Commun. Conf. Postdeadline Papers*, OSA Technical Digest (online) (Optica Publishing Group, 2018, paper Th4B.3.

[44] C. Koebele et al., "Two mode transmission at 2x100 Gb/s, over 40 km-long prototype few-mode fiber, using LCOS-based programmable mode multiplexer and demultiplexer," *Opt. Exp.*, vol. 19, no. 17, pp. 16593–16600, 2011. [Online]. Available: https://opg.optica.org/oe/abstract.cfm?uri=oe-19-17-16593

[45] D. Flamm, D. Naidoo, C. Schulze, A. Forbes, and M. Duparr, "Mode analysis with a spatial light modulator as a correlation filter," *Opt. Lett.*, vol. 37, no. 13, pp. 2478–2480, 2012. [Online]. Available: https://opg.optica.org/ol/abstract.cfm?uri=ol-37-13-2478

[46] Q. Chen et al., "Soft mesocrystal enabled multi-degree light modulation," *Laser Photon. Rev.*, vol. 18, no. 5, 2024, Art. no. 2301283.

[47] HOLOEYE photonics AG. (n.d.). [Online]. Available: https://holoeye.com/

[48] Meadowlark optics. (n.d.). [Online]. Available: https://www.meadowlark.com/

[49] D. Dai et al., "10-channel mode (de)multiplexer with dual polarizations," *Laser Photon. Rev.*, vol. 12, no. 1, 2018, Art. no. 1700109, doi: 10.1002/lpor.201700109. [Online]. Available: https://onlinelibrary.wiley.com/doi/abs/10.1002/lpor.201700109

[50] A. Annoni et al., "Unscrambling light automatically undoing strong mixing between modes," *Light: Sci. Appl.*, vol. 6, no. 12, 2017, Art. no. e17110. [Online]. Available: https://www.nature.com/articles/lsa2017110

[51] K. R. Mojaver, S. M. R. Safaee, S. S. Morrison, and O. Liboiron-Ladouceur, "Recent advancements in mode division multiplexing for communication and computation in silicon photonics," *J. Lightw. Technol*, vol. 42, no. 22, pp. 7860–7870, Nov. 2024. [Online]. Available: https://ieeexplore.ieee.org/document/10553309/?arnumber=10553
309

[52] J. Wang, S. He, and D. Dai, "On-chip silicon 8-channel hybrid (de)multiplexer enabling simultaneous mode- and polarization-division-multiplexing," *Laser Photon. Rev.*, vol. 8, no. 2, pp. L18–L22, 2014, doi: 10.1002/lpor.201300157, [Online]. Available: https://onlinelibrary.wiley.com/doi/abs/10.1002/lpor.201300157

[53] W. Chang et al., "Ultra-compact mode (de) multiplexer based on subwavelength asymmetric Y-junction," *Opt. Exp.*, vol. 26, no. 7, pp. 8162–8170, 2018. [Online]. Available: https://opg.optica.org/abstract.cfm?URI=oe-26-7-8162

[54] W. Jiang, S. Mao, J. Hu, J. Wang, and H. Wan, "Inverse design and demonstration of on-chip silicon high-order mode pass filter," *APL Photon.*, vol. 9, no. 2, 2024, Art. no. 021301. [Online]. Available: https://doi.org/10.1063/5.0169729

[55] B. Stern et al., "On-chip mode-division multiplexing switch," *Optica*, vol. 2, no. 6, pp. 530–535, 2015. [Online]. Available: https://opg.optica.org/optica/abstract.cfm?uri=optica-2-6-530

[56] Y. Xiong, R. B. Priti, and O. Liboiron-Ladouceur, "High-speed two-mode switch for mode-division multiplexing optical networks," *Optica*, vol. 4, no. 9, pp. 1098–1102, 2017. [Online]. Available: https://opg.optica.org/abstract.cfm?URI=optica-4-9-1098

[57] L. Yang et al., "General architectures for on-chip optical space and mode switching," *Optica*, vol. 5, no. 2, pp. 180–187, 2018. [Online]. Available: https://opg.optica.org/abstract.cfm?URI=optica-5-2-180

[58] C. D. Truong, D. Nguyen Thi Hang, H. Chandrahalim, and M. T. Trinh, "On-chip silicon photonic controllable 2 x 2 four-mode waveguide switch," *Sci. Rep.*, vol. 11, no. 1, 2021, Art. no. 897. [Online]. Available: https://www.nature.com/articles/s41598-020-80174-8

[59] L.-W. Luo et al., "WDM-compatible mode-division multiplexing on a silicon chip," *Nature Commun.*, vol. 5, no. 1, 2014, Art. no. 3069. [Online]. Available: https://www.nature.com/articles/ncomms4069

[60] S. Wang et al., "On-chip reconfigurable optical add-drop multiplexer for hybrid wavelength/mode-division-multiplexing systems," *Opt. Lett.*, vol. 42, no. 14, pp. 2802–2805, 2017. [Online]. Available: https://opg.optica.org/abstract.cfm?URI=ol-42-14-2802

[61] W. Zhao et al., "96-channel on-chip reconfigurable optical add-drop multiplexer for multidimensional multiplexing systems," *Nanophotonics*, vol. 11, no. 18, pp. 4299–4313, 2022. [Online]. Available: https://www.degruyter.com/document/doi/10.1515/nanoph-2022-0319/html?lang=en&srsltid=AfmBOorZriYiuqciMkg_mRFuMqve6Ek8Do-0o7f9iOvb94R35oh2FZO9

[62] W. T. Welford, R. Winston, and D. C. Sinclair, "The optics of nonimaging concentrators: Light and solar energy," *Phys. Today*, vol. 33, no. 6, pp. 56–57. [Online]. Available: https://doi.org/10.1063/1.2914121

[63] J. C. C. Mak, W. D. Sacher, H. Ying, X. Luo, P. G. -Q. Lo, and J. K. S. Poon, "Multi-layer silicon nitride-on-silicon polarization-independent grating couplers," *Opt. Exp.*, vol. 26, no. 23, pp. 30623–30633, 2018. [Online]. Available: https://opg.optica.org/abstract.cfm?URI=oe-26-23-30623

[64] J. Hong, A. M. Spring, F. Qiu, and S. Yokoyama, "A high efficiency silicon nitride waveguide grating coupler with a multilayer bottom reflector," *Sci. Rep.*, vol. 9, no. 1, 2019, Art. no. 12988. [Online]. Available: https://www.nature.com/articles/s41598-019-49324-5

[65] V. Vitali, C. Lacava, T. Dominguez Bucio, F. Y. Gardes, and P. Petropoulos, "Highly efficient dual-level grating couplers for silicon nitride photonics," *Sci. Rep.*, vol. 12, no. 1, 2022 Art. no. 15436. [Online]. Available: https://www.nature.com/articles/s41598-022-19352-9

[66] W. Fraser et al., "High-efficiency self-focusing metamaterial grating coupler in silicon nitride with amorphous silicon overlay," *Sci. Rep.*, vol. 14, no. 1, 2024, Art. no. 11651. [Online]. Available: https://www.nature.com/articles/s41598-024-62336-0

[67] S. Ghosh, S. Yegnanarayanan, D. Kharas, M. Ricci, J. J. Plant, and P. W. Juodawlkis, "Wafer-scale heterogeneous integration of thin film lithium niobate on silicon-nitride photonic integrated circuits with low loss bonding interfaces," *Opt. Exp.*, vol. 31, no. 7, 2023, pp. 12005–12015. [Online]. Available: https://opg.optica.org/oe/abstract.cfm?uri=oe-31-7-12005

[68] Y. Tan et al., "Micro-transfer printed thin film lithium niobate (TFLN)-on-silicon ring modulator," *ACS Photon.*, vol. 11, no. 5, pp. 1920–1927, 2024. [Online]. Available: https://doi.org/10.1021/acsphotonics.3c01869

[69] S. Abel et al., "A strong electro-optically active lead-free ferroelectric integrated on silicon," *Nature Commun.*, vol. 4, no. 1, 2013, Art. no. 1671. [Online]. Available: https://www.nature.com/articles/ncomms2695

[70] P. Stark et al., "Heterogeneous co-integration of BTO/Si and III-V technology on a silicon photonics platform," in *Proc. Opt. Fiber Commun. Conf. Exhib.*, 2020, pp. 1–3. [Online]. Available: https://ieeexplore.ieee.org/document/9083294

[71] W. Guo, A. B. Posadas, and A. A. Demkov, "Epitaxial integration of $BaTiO_3$ on Si for electro-optic applications," *J. Vac. Sci. Technol. A*, vol. 39, no. 3, 2021, Art. no. 030804, doi: 10.1116/6.0000923.

[72] P. Prabhathan et al., "Roadmap for phase change materials in photonics and beyond," *iScience*, vol. 26, no. 10, 2023, Art. no. 107946. [Online]. Available: https://www.sciencedirect.com/science/article/pii/S2589004223020230

[73] A. Shafiee, B. Charbonnier, J. Yao, S. Pasricha, and M. Nikdast, "Programmable phase change materials and silicon photonics co-integration for photonic memory applications: A systematic study," *Proc. SPIE*, vol. 4, no. 3, 2024, Art. no. 031208.

[74] N. Quack et al., "Integrated silicon photonic MEMS," *Microsyst Nanoeng*, vol. 9, no. 27, 2023. [Online]. Available: https://doi.org/10.1038/s41378-023-00498-z

[75] C. Sun, "A 45 nm CMOS-SOI monolithic photonics platform with bit-statistics-based resonant microring thermal tuning," *IEEE J. Solid-State Circuits*, vol. 51, no. 4, pp. 893–907, Apr. 2016. [Online]. Available: https://ieeexplore.ieee.org/document/7426337/?arnumber=7426337

[76] V. Stojanović et al., "Monolithic silicon-photonic platforms in state-of-the-art CMOS SOI processes [invited]," *Opt. Exp.*, vol. 26, no. 10, pp. 13106–13121, 2018. [Online]. Available: https://opg.optica.org/abstract.cfm?URI=oe-26-10-13106

[77] F. Zanetto et al., "Time-multiplexed control of programmable silicon photonic circuits enabled by monolithic CMOS electronics," *Laser Photon. Rev.*, vol. 17, no. 11, 2023, Art. no. 2300124, doi: 10.1002/lpor.202300124. [Online]. Available: https://onlinelibrary.wiley.com/doi/abs/10.1002/lpor.202300124

[78] F. Zanetto et al., "Unconventional monolithic electronics in a conventional silicon photonics platform," *IEEE Trans. Electron Devices*, vol. 70, no. 10, pp. 4993–4998, Oct. 2023. [Online]. Available: https://ieeexplore.ieee.org/abstract/document/10226459

[79] W. R. Clements, P. C. Humphreys, B. J. Metcalf, W. S. Kolthammer, and I. A. Walmsley, "Optimal design for universal multiport interferometers," *Optica*, vol. 3, no. 12, pp. 1460–1465, 2016. [Online]. Available: https://opg.optica.org/optica/abstract.cfm?uri=optica-3-12-1460

[80] F. Marchesin et al., "Braided interferometer mesh for robust photonic matrix-vector multiplications with non-ideal components," *Opt. Exp.*, vol. 33, no. 2, pp. 2227–2246, 2025. [Online]. Available: https://opg.optica.org/abstract.cfm?URI=oe-33-2-2227

[81] M. Milanizadeh et al., "Separating arbitrary free-space beams with an integrated photonic processor," *Light Sci. Appl.*, vol. 11, no. 1, 2022, Art. no. 197. [Online]. Available: https://doi.org/10.1038/s41377-022-00884-8

[82] A. Li, Y. Wang, J. Fang, M.-J. Li, B. Y. Kim, and W. Shieh, "Few-mode fiber multi-parameter sensor with distributed temperature and strain discrimination," *Opt. Lett.*, vol. 40, no. 7, pp. 1488–1491, 2015. [Online]. Available: https://opg.optica.org/ol/abstract.cfm?uri=ol-40-7-1488

[83] I. Ashry et al., "A review of using few-mode fibers for optical sensing," *IEEE Access*, vol. 8, pp. 179592–179605, 2020. [Online]. Available: https://ieeexplore.ieee.org/document/9209959/?arnumber=9209959

[84] C. Roques-Carmes, S. Fan, and D. A. B. Miller, "Measuring, processing, and generating partially coherent light with self-configuring optics," *Light: Sci. Appl.*, vol. 13, no. 1, Sep. 2024, Art. no. 260. [Online]. Available: https://doi.org/10.1038/s41377-024-01622-y

[85] D. Sirbu et al., "AstroPIC: Near-infrared photonic integrated circuit coronagraph architecture for the Habitable Worlds Observatory," *Proc. SPIE*, vol. 13092, 2024, Art. no. 130921T. [Online]. Available: https://doi.org/10.1117/12.3020518

[86] S. SeyedinNavadeh et al., "Integrated mode-selective repeater for free-space optical communications," in *Proc. 25th Eur. Conf. Integr. Opt.*, J. Witzens, J. Poon, L. Zimmermann, and W. Freude, Eds., Springer Nature Switzerland, 2024, pp. 309–314.

[87] H. Rubinsztein-Dunlop et al., "Roadmap on structured light," *J. Opt.*, vol. 19, no. 1, 2016, Art. no. 013001. [Online]. Available: https://dx.doi.org/10.1088/2040-8978/19/1/013001

[88] I. Cristiani et al., "Roadmap on multimode photonics," *J. Opt.*, vol. 24, no. 8, 2022, Art. no. 083001. [Online]. Available: https://dx.doi.org/10.1088/2040-8986/ac7a48

[89] M. Ghalaii and S. Pirandola, "Quantum communications in a moderate-to-strong turbulent space," *Commun. Phys.*, vol. 5, no. 1, pp. 1–12, 2022. [Online]. Available: https://www.nature.com/articles/s42005-022-00814-5

[90] M. Verde, C. T. Schmiegelow, U. Poschinger, and F. Schmidt-Kaler, "Trapped atoms in spatially-structured vector light fields," *Sci. Rep.*, vol. 13, no. 1, 2023, Art. no. 21283. [Online]. Available: https://www.nature.com/articles/s41598-023-48589-1

[91] C. Li, A. Tsourdos, and W. Guo, "A transistor operations model for deep learning energy consumption scaling law," *IEEE Trans. Artif. Intell.*, vol. 5, no. 1, Jan. 2024, pp. 192–204, doi: 10.1109/TAI.2022.3229280.